

Effective temperature of amorphous carbon studied using nuclear-resonance photon scattering

R. Moreh

Physics Department, Ben-Gurion University of the Negev, Beer-Sheva 84105, Israel

O. Beck and D. Jäger

Institut für Strahlenphysik, Universität Stuttgart, D-70569 Stuttgart, Germany

Y. Finkelstein

Physics Department, Ben-Gurion University of the Negev, Beer-Sheva 84105, Israel

U. Kneissl, J. Margraf, H. Maser, and H. H. Pitz

Institut für Strahlenphysik, Universität Stuttgart, D-70569 Stuttgart, Germany

(Received 7 November 1996)

The effective temperature of isotopic amorphous carbon (^{13}C) was measured, at 295 K, by employing the nuclear resonance photon scattering (NRPS) technique. The photon beam was in the form of bremsstrahlung obtained from an electron beam of the Stuttgart Dynamitron, with $E=4.1$ MeV, and the resonance scattering from the 3089-keV and the 3684-keV levels in ^{13}C was measured. The effective temperature of ^{13}C was found to be (822 ± 123) K, which is higher by about 13% than that calculated from the experimental vibrational density of states of amorphous carbon. This deviation is discussed. [S0163-1829(97)01925-5]

I. INTRODUCTION

In the present work, we measure the effective temperature of the C atoms in amorphous carbon (AC) by applying the nuclear resonance photon scattering (NRPS) technique in a self-absorption mode.^{1,2} The effective temperature T_s is related to the *total* kinetic energy of the C atom. This, in turn, is related to the average binding forces acting on each atom. In the NRPS method, one monitors the Doppler broadening of the nuclear level caused by the *total* kinetic energy of the scattering C atom. It turns out that the scattered intensity is related to the directional binding strength of the scattering atoms. The Doppler width is given by $\Delta_s = E(2kT_s/M_s c^2)^{1/2}$ where E is the nuclear level energy, M_s is the nuclear mass, and T_s is the effective temperature of the scattering atom; it is related to its *total* kinetic energy in the sense that it includes the part which is due to its internal zero-point motion. At low temperatures, the main contribution to the Doppler broadening arises mainly from the kinetic energy of the zero-point vibrational motion of the C atoms. In the present work we use the 4.1-MeV bremsstrahlung beam of the University of Stuttgart to determine T_s by measuring the resonance photon scattering of the 3089- and the 3684-keV levels in ^{13}C .

Amorphous carbon (AC) is one of several forms of elemental carbon which also occurs in a crystalline form such as graphite, diamond, and fullerenes. Graphite is known to be highly anisotropic and to have a hexagonal planar structure and strong covalent trigonal bonds (sp^2) with an interatomic distance of 0.1415 nm. The fourth electron in the outer shell (in graphite) is responsible for the weak van der Waals binding between the hexagonal planes. The diamond crystal structure is face-centered cubic with interatomic distances of 0.154 nm and each atom is covalently bonded to four other carbon atoms, sp^3 , tetragonal bonds. In fullerenes,

such as C_{60} , each molecule consists of 12 pentagons and 20 hexagons with a nearly spherical cage-shaped form. This is a molecular solid crystal belonging to a face-centered-cubic phase. The covalent bond holding each C atom is nearly trigonal and close to that of graphite.

AC may have either sp^3 - or sp^2 -type bonds or a combination of both. The first is termed diamond-like and the second graphitelike AC. Raman spectroscopy and many other techniques are used for characterizing the particular type of AC.

This nuclear technique was applied previously to pyrolytic BN where the anisotropic resonance scattering from five nuclear levels below 9 MeV in ^{11}B was measured.¹ It was later applied to ^{39}K levels using 8.5-MeV bremsstrahlung² where the anisotropic binding of the K atoms in the graphite intercalated compound C_8K was studied. In the present work we apply the NRPS method to study the binding effects of C atoms by utilizing the nuclear properties of the two nuclear levels^{3,4} in ^{13}C .

The present work was motivated by the results of some investigators⁵⁻⁷ who used the neutron Compton scattering (NCS) method to measure the effective temperatures of graphite in directions parallel and perpendicular to the hexagonal layers and to test the lattice dynamical calculations of the phonon spectrum of graphite. A large deviation between the measured and calculated values was observed for the effective temperature parallel to the graphite layers. It was thus very interesting to measure the effective temperature of carbon in a related sample, namely in AC, using an entirely different method to find out whether such deviation will also occur using the present technique.

II. THE NRPS TECHNIQUE

This method is illustrated (for the case of the ^{13}C isotope) in Fig. 1 which depicts an incident bremsstrahlung beam

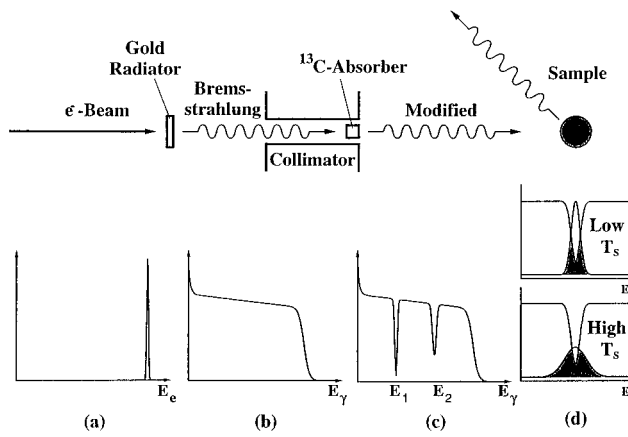


FIG. 1. The upper part describes the sequence of events in a NRPS experiment while the corresponding energy spectra of electrons and photons are depicted in the lower part. The electron beam (a) hits the gold radiator target and produces a bremsstrahlung photon spectrum (b). The passage of this photon beam through the nuclear self-absorber generates the Doppler broadened dips in the continuous bremsstrahlung spectrum corresponding to the excitations of the two nuclear levels in ^{13}C (c). The scattered intensities of the modified bremsstrahlung incident on the sample depends on the overlap integrals [shown as shaded areas in (d)] between the Doppler broadened shapes of the dips and of the nuclear levels in the scatterer, and are shown in part (d) for cases of low and high T_s .

obtained when 4.1 MeV electrons strike a high-Z gold radiator. This 4.1-MeV incident “white” beam is modified by passing it through an absorber (containing ^{13}C nuclei) which generates narrow nuclear absorption dips caused by the excitation of the 3089- and the 3684-keV levels in ^{13}C . The particular shape and width of those dips which are Doppler broadened are determined by the atomic binding properties of the ^{13}C absorber. Similarly, the levels of the scatterer are also Doppler broadened with widths defined above. The shapes of those lines carry the lattice dynamical information of the scattering atoms, which is of our concern here. When this artificially modified photon beam strikes a nuclear scatterer (containing ^{13}C nuclei), the Doppler broadened dips that were created by the absorber act as shape analyzers of the broadened levels of the scatterer. The overlap of the two shapes (described by the shaded areas in Fig. 1) is proportional to the scattered intensity which, in turn, depends on the effective temperature of the scatterer. For two ^{13}C samples with different effective temperatures ($T_1 < T_2$) which are struck by the above artificially modified beam, the corresponding scattered intensities I_1, I_2 will also be different, namely, $I_1 < I_2$. The overlap integrals describing the scattering process are illustrated as the shaded areas in the drawings shown at the bottom of the right-hand corner of Fig. 1 for the two different samples.

It should be stressed that, in principle, it is possible to get the same information by scattering from the 4439-keV level in ^{12}C which is the abundant isotope of carbon (98.89%). This level is, however, not suitable for this application first because its energy is higher than accessible at the Stuttgart Dynamitron and because its radiative width³ is small ($\Gamma_0 = 0.011$ eV) and the resulting dependence of the scattering

intensity on effective temperature (in the special configuration of Fig. 1) is expected to be quite weak. Thus the use of ^{13}C is preferable mainly due to the much larger widths of the ^{13}C nuclear levels which increases by far the scattering intensity and also because of the lower excitation energies of its nuclear levels. In fact, the radiative widths⁴ of the 3089- and the 3684-keV levels in ^{13}C are around $\Gamma_0 = 0.5$ eV and are much smaller than the corresponding Doppler widths being $\Delta \sim 12$ and 14 eV, respectively. The two conditions, namely, a large Γ_0 combined with the requirement $\Gamma_0 \ll \Delta$ make the two levels in ^{13}C an ideal choice for studying the binding properties of C-containing systems. This also ensures higher sensitivity of the scattering cross section to variations in the Doppler width and hence to temperature and orientational changes of the scatterer with respect to the photon beam. It is also important to note that a large Γ_0 fulfills another basic requirement inherent in the present technique namely a very *short lifetime* of the nuclear level. This condition is of absolute necessity because it ensures that no slowing down of the recoil nucleus occurs before reemitting the scattered photon and hence no attenuation of the Doppler broadening of the nuclear level can take place in such a process. The level lifetime τ should be much shorter than the interval ($t_0 = 10^{-13}$ s) a recoiling nucleus (of an atom) takes to cross one mean free path in the atomic lattice.

It should be noted that T_s may also be measured using another technique namely, the neutron Compton scattering⁵⁻⁷ (NCS) with neutron energies in the eV range. In this method, neutrons from a pulsed spallation source are scattered at backward angles and the neutron energies are measured using a resonance foil placed in front of the detector. By analyzing the energy spread of the scattered neutrons using time of flight, it is possible to determine the atomic momentum distributions of the scattering atoms in the sample. However, the determination of T_s by this method relies on calculating the scattering amplitude of the neutrons using the impulse approximation and on estimating the final-state effects. Hence this method is model dependent. Some of the T_s results obtained using this method are discussed in Sec. V.

A different version of the NRPS method based on monoenergetic photon beams generated by (n, γ) reactions was also used for studying effective temperatures.⁸⁻¹¹ The results obtained with the (n, γ) method are quite accurate and required relatively shorter running times. However, its applicability is restricted to only few isotopes such as ^{15}N , ^{68}Zn , and ^{62}Ni because the nuclear levels studied were photoexcited by a chance overlap between one γ line of the photon source and a nuclear level in the scatterer.⁸ This fact reduced substantially the number of cases which could be studied by this technique.

III. THEORETICAL REMARKS

A. Scattered intensities and self-absorption ratios

In the present technique, one creates a dependence of the scattered intensity on the effective temperature T_s of the scatterer by using a nuclear self-absorber. This dependence is eventually used for the determination of T_s . In calculating the scattered intensity we have to account for the thicknesses of the nuclear absorber and the scatterer, their isotopic abun-

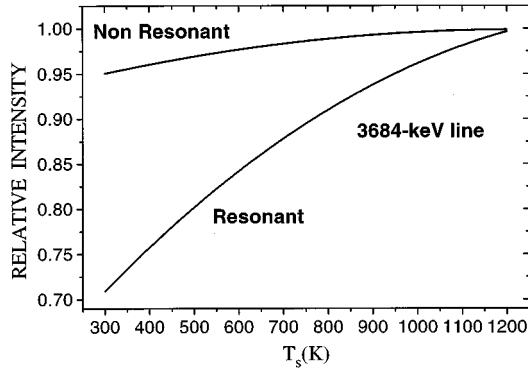


FIG. 2. Calculated relative scattered intensities (normalized to 295 K) from the 3089-keV levels in ^{13}C as a function of T_s , the effective temperature of the scatterer. The lower and upper curves represent the calculated results obtained with and without ^{12}C and ^{13}C absorbers, respectively. The absorber thicknesses were taken to be 3.28 g/cm^2 (^{12}CO) and 3.39 g/cm^2 (^{13}CO) with $T_a = 346 \text{ K}$. Note that the strong dependence of the scattered intensities on T_s occurs only when a ^{13}C absorber is used.

dances, their effective temperatures and hence the Doppler widths, and for the parameters of the nuclear level. The scattered intensity is related to the parameters of the nuclear level through the factor $g\Gamma_0^2/\Gamma$, where Γ_0, Γ are the ground state and the total level widths, and $g = (2J+1)/(2J_0+1)$ is a statistical factor with J and J_0 the spins of the excited and the ground states of ^{13}C . The method of calculating the scattered intensity follows the procedure described in detail elsewhere^{12,13} for a white spectrum passing through a self-absorber and hitting a scatterer. Both the self-absorber and scatterer are thick and the calculation requires numerical integration procedures.

To get an idea about the sensitivity of the present technique for the determination of T_s , we show as an example the calculated scattering intensity from the 3089-keV level as a function of the effective temperature T_s . The results (normalized to unity at $T_s = 1200 \text{ K}$) are plotted in Fig. 2 for two cases: (a) in which the bremsstrahlung beam passes through a 3.390 g/cm^2 ^{13}CO nuclear absorber (assumed to be in a liquid form at 78 K and whose effective temperature is $T_a = 346 \text{ K}$) before hitting the target, and (b) the beam passes through a pure nonresonant ^{12}CO absorber (of equivalent atomic thickness to that of the ^{13}CO absorber) before striking the sample. The nuclear absorption of the 3089-keV line caused by a 1.50 g/cm^2 of ^{13}C absorber contained in liquid ^{13}CO is 37.4%.

In Fig. 2, the thickness of the AC sample is 0.429 g/cm^2 and is equal to that used in the present work. It may be seen that while the upper curve of Fig. 2 has only a slight dependence on T_s , the lower curve increases strongly with T_s . This dependence may be qualitatively understood by considering Fig. 1. Here, the shaded areas under the overlapping lines represent the scattering cross section, from which it is easy to see that when the Doppler broadening of the scattering line is small, the overlap integral (represented by the shaded area in Fig. 1) becomes smaller leading to a strong dependence on T_s . The slight variation with T_s of the upper curve is caused by the nuclear self-absorption in the ^{13}C sample itself which has a finite thickness and acts as a nuclear absorber.

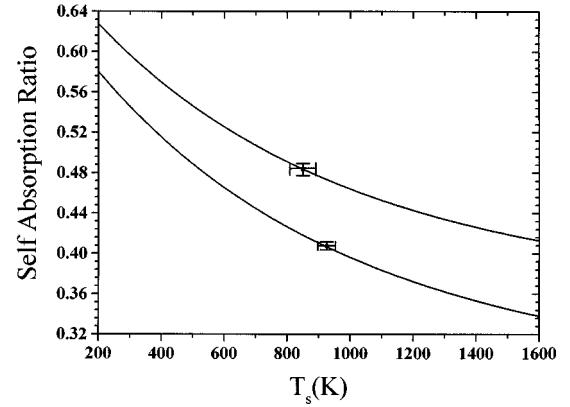


FIG. 3. The calculated self-absorption ratio R of the 3089-keV level as a function of the effective temperature T_s of the scatterer. The ^{13}C scatterer thickness was taken to be 0.429 g/cm^2 with a 3.43-g/cm^2 -thick liquid ^{13}CO absorber. The upper curve represents the results obtained with no comparative absorber while the lower curve represents the results obtained using a comparative ^{12}CO absorber, 3.38 g/cm^2 thick.

Experimentally, it is much easier to measure the self-absorption ratio R from any resonance scattering level. This ratio is defined as $R = (N_0 - N_n)/N_0$ with N_n and N_0 , the scattered intensities from the sample obtained by passing the incident photons through a resonant and a nonresonant absorber, containing ^{13}C and ^{12}C , respectively before hitting the sample. In such measurements, the thicknesses of the resonant and nonresonant absorbers are usually chosen to have the same atomic attenuation. Such ratios are calculated by utilizing the results of the lower curve of Fig. 2 and the values of R versus T_s are plotted in Fig. 3 for the 3089-keV scattering level. Figure 3 shows that R increases with decreasing T_s . This means that a higher experimental self-absorption ratio R is obtained if one uses a nuclear self-absorber with a low T_s . This also means that a better sensitivity to changes in T_s may be achieved if one uses a nuclear absorber with low effective temperature such as liquid ^{13}CO , as will be discussed in detail below.

B. Effective temperatures

The effective temperature of the C atoms which is of our concern here is related to the *total* kinetic energy of the atoms. In cases where the phonon spectrum of the scatterer is experimentally known, the effective temperature may be calculated. This may be done by integration over the vibrational density of states, $g(\nu)$ with a maximum frequency ν_m using the relation obtained by Lamb:¹⁴

$$T_s = \frac{(1/k) \int_0^{\nu_m} g(\nu) \alpha h \nu d\nu}{\int_0^{\nu_m} g(\nu) d\nu}, \quad (1)$$

where $\alpha = [(e^{h\nu/kT} - 1)^{-1} + 0.5]$ and k is the Boltzmann constant.

In the literature, the only calculation of the vibrational density of states of amorphous carbon which we know about is that by Kamitakahara¹⁵ who measured the

inelastic scattering of a sputtered amorphous carbon sample and also of glassy carbon. It turned out, however, as will be seen in Sec. V, that the effective temperatures of the C atoms in graphite is close to within 5% to that of the other types of carbon, namely, AC and glassy carbon which is widely regarded as nanocrystalline graphitic material.

As noted earlier, it is very difficult to measure with good accuracy the *absolute* scattered photon intensities which could yield the effective temperatures. Rather, it is preferable to measure the ratios of the scattered intensities, such as the self-absorption ratio R , which involve a much smaller experimental error leading to higher precision in the determination of the effective temperature. The calculation of R involves a knowledge of the nuclear parameters T_s , T_a , Γ_0 , and Γ . Hence by measuring R , one can determine T_s if T_a , Γ and Γ_0 are known. Alternatively, T_a may be determined if T_s , Γ and Γ_0 are known. We thus determined the effective temperature T_s of AC by two separate measurements of R . In the first, we used AC both as scatterer and absorber; thus deducing $T_s = T_a$ by an iterative procedure. In the second, a liquid ^{13}C absorber was employed in conjunction with an AC scatterer and T_s could be deduced because the value of T_a of ^{13}C (in liquid ^{13}C) could be calculated. This was done by following the procedure used in calculating the effective temperature of the N-atom^{9,16} in $^{15}\text{N}_2$ where an excellent agreement was obtained between the calculated and measured value of T_s .

To calculate the effective temperature T_a of ^{13}C in a solid ^{13}CO , we note that¹⁶

$$(3/2)kT_a = (3/2)S_t kT_t + S_r kT_r + (1/2)S_v h\nu\alpha_0, \quad (2)$$

where S_t , S_r , and S_v are the kinetic-energy fractions of the translational, rotational, and the internal vibrational motions shared by the C atom in the CO molecule. T_t and T_r are the effective temperatures of the translational and rotational motions. Thus, $S_t = (13/29)$, and $S_r = S_v = (16/29)$. The factor (3/2) on the right-hand side of Eq. (2) is contributed by the three kinetic degrees of freedom of the C atom in the CO molecule, where each degree of freedom is assigned a kinetic energy $kT_a/2$ while the factor (1/2) in the last term of Eq. (2) arises from the fact that only the kinetic part of the internal vibrational energy ($h\nu_0$) contributes to the Doppler broadening of the nuclear level and hence to T_a . The internal vibrational frequency of the ^{13}CO molecule, $\nu_0 = 2092.3 \text{ cm}^{-1}$ was taken from infrared measurements.¹⁷ Substituting the above values in Eq. (2) and using the same effective temperature for the translational and rotational motion, namely $T_t = T_r$, we get

$$T_a = 0.8161T_t + 276.8, \quad (3)$$

where the 276.8 K in Eq. (3) is contributed by the zero-point energy of the internal vibrational motion of the CO molecule. It should be noted that T_t is related to the distribution of frequencies, $g(\nu)$, of the translational and rotational motions of the entire CO molecule in the solid or liquid phase. For a Debye-type solid, $g(\nu) = 3\nu^2/\nu_m^3$ (with ν_m the cutoff frequency related to the Debye temperature, $\Theta_0 = h\nu_m/k$, of the molecular CO solid lattice, known¹⁸ to be $\Theta = 103 \text{ K}$. T_t may be expressed by the Lamb relation¹⁴ deduced under the harmonic approximation

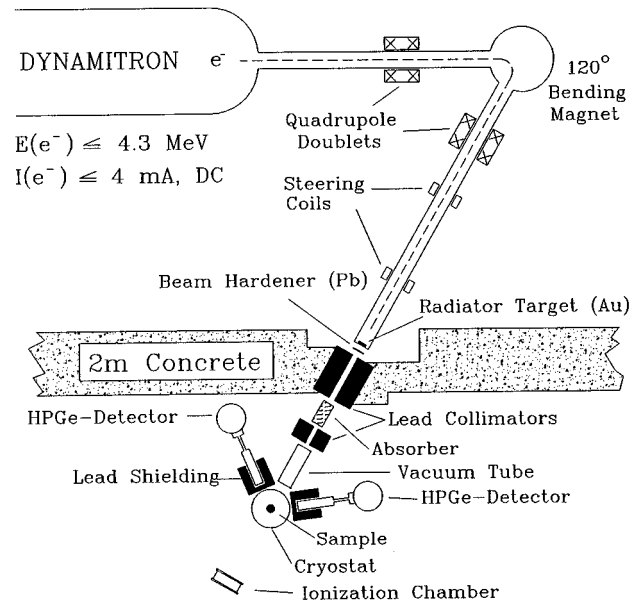


FIG. 4. Sketch of the bremsstrahlung facility installed at the Stuttgart Dynamitron accelerator (Ref. 19). The bremsstrahlung beam, produced by the bombardment of the radiator target by the high-intensity electron beam of the Dynamitron, is collimated and passed through an absorber before hitting the scattering sample in the experimental area. The photon beam intensity is monitored during the measurement by an ionization chamber.

$$T_t = \frac{T^4}{\Theta^3} \int_0^{\Theta/T} x^3 \left[\frac{1}{\exp(x) - 1} + \frac{1}{2} \right] dx \quad (4)$$

with $x = (h\nu/kT)$. At $T = 78 \text{ K}$ (which is the assumed temperature of liquid N_2 used for cooling the CO absorber), we get $T_t = 84.6 \text{ K}$ and using Eq. (3), we get $T_a = 345.9 \text{ K}$. The increment of T_a above 78 K expresses the total contributions of the zero-point energies of the internal vibrations, the intramolecular vibrations and the librational motion of the CO molecules in the *solid* phase. In the present work, we apply the same effective temperature for a molecular liquid; the validity of this last assumption was established in the case of N_2 .

IV. EXPERIMENTAL DETAILS

The bremsstrahlung is generated when a 4.1-MeV beam of electrons strikes a 4-mm-thick water-cooled gold radiator which ensures a complete stopping of the electron beam. A schematic diagram of the experimental setup is shown in Fig. 4. The electron beam is obtained from the 100% duty cycle Dynamitron accelerator of the University of Stuttgart¹⁹ whose current varied between 150 and 250 μA on the radiator. The electron beam is first passed through a 120° bending magnet and focused on the Au radiator. The produced bremsstrahlung beam is then passed through a 3-mm lead hardener, to a 1-m-long lead collimator containing a 1.0 cm through hole (which leads to the experimental area), and then to a nuclear absorber before hitting the sample. For detecting the scattered radiation, two hyperpure germanium (HPGe) detectors were used, at scattering angles of 115° and 125° (with efficiencies of 99% and 31%) and were placed at dis-

tances of 22 and 19 cm from the geometrical center of the target. Photon hardeners consisting of lead (2.5 cm) were placed in front of the 115° detector. Around the 125° detector, the hardener thicknesses were lead (1.6 cm). These hardeners attenuated markedly the low-energy scattered radiation. The gamma-ray energy resolution of the detectors was 4.2 keV at 3864 keV. Other details of the experimental system, the electronics and data acquisition method, were described elsewhere.¹⁹

The ¹³C AC sample was in a powder form encapsulated inside a thin-walled plastic container and packed to form a cylindrical sample with its axis in the scattering plane and having an effective thickness of 0.43 g/cm².

During the photon-scattering measurements, the AC sample was kept inside an evacuated tube to reduce the background radiation arising from scattering by air molecules. The ends of the tube were provided with thin Mylar windows which were not “seen” by the detectors.

For measuring the nuclear self-absorption effect, it was necessary to detect the scattered radiation from the ¹³C AC sample, first with an isotopically enriched liquid ¹³CO absorber and then using a natural CO absorber (containing 98.89% ¹²C and 1.11% ¹³C), and having the same effective weight as that of the resonant ¹³C absorber. A short background measurement was also carried out using a natural AC sample containing an equivalent amount of natural carbon. All sets of measurements were taken with the AC samples at room temperature and with the liquid CO absorbers at liquid-nitrogen temperature (78 K). The electron beam, the bremsstrahlung, the collimators, and the absorbers were very carefully aligned so that the bremsstrahlung beam could pass in its entirety through the absorber before striking the sample. This was necessary because any fraction of the primary beam which could reach the sample without passing through the absorber, may severely distort the self-absorption measurement.

The liquid ¹³CO absorber was inserted inside a cylindrical stainless-steel container forming a thickness of 3.43 g/cm². The absorbers were prepared by passing the gas using a transfer system, and liquefying it inside the stainless-steel container (15 mm diameter, 42 mm long, 1 mm thick) placed at the bottom of a tall Dewar, (60 cm) filled with liquid nitrogen. This arrangement allowed us to make 8-h runs before refilling with liquid nitrogen. The geometry of the system was such that the amount of liquid nitrogen in the path of the bremsstrahlung beam was negligible compared to the amount of the absorber. Care was taken to assure that no bubbles of gas are left inside the liquid CO absorber. An on-line gas handling system was constructed which could replace the enriched ¹³CO with natural CO absorber.

One of the main sources of error in such measurements arises from small electronic drifts in the end-point energy of the electron beam. This could cause a relatively large change in the resulting bremsstrahlung intensity. To minimize such effects, great care was taken to stabilize the energy of the electron beam. In addition, the measurements of the scattered intensities were repeated several times while interchanging the absorbers. Moreover, the bremsstrahlung beam intensity was monitored using a standard ionization chamber. The total running time for such a measurement in which different

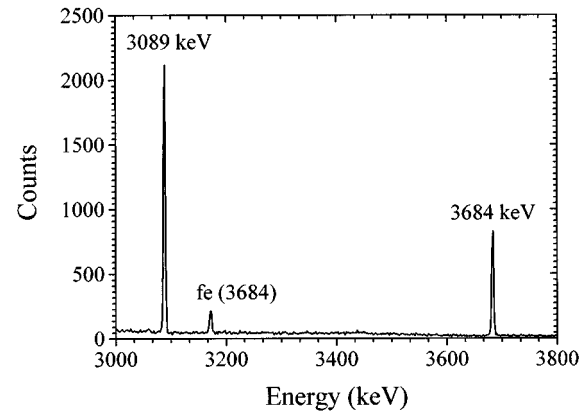


FIG. 5. Typical scattered radiation spectrum from a ¹³C-enriched AC sample as obtained using a 99% hyperpure Ge (HPGe) detector placed at an angle of 115° with respect to the incident bremsstrahlung beam. A hardener consisting of 2.5-cm lead and placed in front of the detector was used for filtering out the low-energy photons.

absorber and scatterer combinations were used is of the order of 14 days.

V. RESULTS AND DISCUSSION

A typical scattered radiation spectrum from a ¹³C AC sample placed in a plastic cylinder as measured using a 99% hyperpure germanium detector (HPGe) is given in Fig. 5 and shows the γ lines corresponding to nuclear resonance scattering from the two levels in ¹³C. The self-absorption ratio is deduced as mentioned in Sec. III A by measuring the scattered intensities after passing the bremsstrahlung beam through a resonant and a nonresonant absorber before hitting the sample. The intensities of the scattered lines were normalized to the measuring time and controlled by the accumulated total charge of the ionization chamber, then corrected for counting losses. The scattering cross-section ratios were extracted for each level by utilizing the intensities of the full energy peak and first-escape peaks of the experimental spectra.

For the case where the absorber was amorphous carbon (2.424 g/cm²) with a scatterer of (0.369 g/cm²), the measured self-absorption was found to be

$$R = 0.546 \pm 0.010 \quad (\text{for the 3089-keV level}),$$

$$R = 0.511 \pm 0.012 \quad (\text{for the 3684-keV level}).$$

This means that by using a 2.424-g/cm²-thick ¹³C AC nuclear absorber, the intensity of the 3684-keV scattered line is 49% of that obtained with a nonresonant absorber. It may be seen that the corresponding atomic attenuation is 8.9%. Combining these data with the calculated values of R of Fig. 3, the effective temperatures of ¹³C in AC, at $T = 295$ K, is extracted yielding

$$T_s = (814 \pm 36) \text{ K}.$$

The corresponding measured self-absorption using the same AC scatterer and a 3.4-g/cm²-thick liquid ¹³CO absorber at 78 K was found to be

$$R = 0.408 \pm 0.004 \quad (\text{for the 3089-keV level}),$$

$$R = 0.370 \pm 0.005 \quad (\text{for the 3684-keV level}).$$

The corresponding measured self-absorption ratios with no atomic absorber were

$$R = 0.483 \pm 0.006 \quad (\text{for the 3089-keV level}),$$

$$R = 0.450 \pm 0.008 \quad (\text{for the 3684-keV level}),$$

yielding another value of T_s at $T = 295$ K,

$$T_s = (906 \pm 22) \text{ K}.$$

The quoted errors in T_s arise only from the statistics of the measurement, and the effect of other factors such as the dependence of T_s on the level width Γ is not included. It turns out that an 8% error in Γ introduces a 16% error in the deduced value of T_s . The large difference between the above two measured values of T_s is not understood. The possibility that the liquid CO absorber contained some bubbles (which tend to increase the resulting value of T_s) was checked by carrying out an independent measurement of its atomic absorption using a radioactive source. We found that this factor cannot explain such a large deviation between the two values. Since there was no reason to prefer any of the above results, we adopt their average, namely,

$$T_s = (859 \pm 38) \text{ K}.$$

Including the uncertainty in Γ_0 increases the error in T_s by about 15%. Thus,

$$T_s = (859 \pm 129) \text{ K}.$$

This is because the values of Γ_0 used for deducing T_s are⁴

$$\Gamma_0(3089 \text{ keV}) = (0.537 \pm 0.042) \text{ eV}$$

and

$$\Gamma_0(3684 \text{ keV}) = (0.403 \pm 0.030) \text{ eV}.$$

The present result was obtained at $T = 295$ K, using isotopic (^{13}C) AC; the corresponding value for a natural AC sample containing 98.9% ^{12}C is deduced by multiplying by the inverse square root of the mass ratio, yielding

$$T_s = (894 \pm 134) \text{ K}.$$

The huge difference between T_s and 295 K is due solely to the effect of the zero-point vibrations of the C atoms. This measured value may be compared with $T_s = 720$ K and $T_s = 743$ K calculated from Eq. (1) at 295 K by using the vibrational density of states (VDOS) of the C atoms in sputtered AC and glassy carbon (which is a form of *nanocrystalline* graphitic carbon) reported by Kamatikahara.¹⁵ It is interesting to note that the above values of T_s are close to those of graphite where the VDOS were reported by Young and Koppel,²⁰ Nicklow *et al.*,²¹ and Al-Jishi and Dresselhaus.²² The corresponding values obtained at 295 K, using Eq. (1), are $T_s = 717$, 773, and 725 K. Our measured value seems to be much higher than the calculated ones. However, by including the uncertainty in the level widths, the measured value of T_s enters within a little more than one standard deviation of the calculated values.

In the literature, some measurements of the effective temperatures of *graphite* were reported at room temperature by Rauh and Watanabe,⁵ Paoli and Holt,⁶ and by Mayers *et al.*⁷ using the neutron Compton scattering method; the results were $T_s = (883 \pm 63)$ K, (834 ± 63) K, and (838 ± 23) K, respectively, which are also higher than the calculated ones. In fact, our measured value for AC is close to the average obtained using the NCS method.

Another remark concerning the width of the ^{13}C levels is in order. In a recent scattering measurement, the width of the two levels was determined using as a reference the known widths of some ^{27}Al levels²³ whose energies are close to those of ^{13}C . An agreement was obtained with the width of the 3684-keV level. However, the width of the 3089-keV level was lower by about 12% than that quoted above. Taking the average of the level widths of the two independent measurements yields $\Gamma_0(3089 \text{ keV}) \sim 0.50$ eV. Using this new level width for analyzing the data of the present work brings down our average measured value to

$$T_s = (822 \pm 123) \text{ K},$$

making it closer to those measured by the NCS method but still higher by about 13% than the predicted values. It would thus be important to make a very accurate measurement of the widths of the nuclear levels in ^{13}C and refine the error in the deduced value of T_s .

The deviation between the measured and calculated T_s could be due, at least partly, to anharmonic contributions to the vibrational energies [neglected in Eq. (1)]; however, the fact that T_s depends primarily on the zero-point energy of the high-energy phonons which are not excited at 295 K would tend to make the anharmonic contribution quite small. This point may be illustrated by noting that a change of the thermodynamic temperature of AC between 295 and 0 K reduces the predicted value of T_s only by 4.7%, namely from 717 K at 295 K, to $T_s = 685$ K at 0 K, hence the anharmonic effects cannot explain a deviation of the order of 13%.

It may also be argued that the deviation is caused by some unknown high-frequency modes in graphite which are not observed yet. This is not very likely, however, because no such modes were observed in graphite when infrared and Raman scattering measurements were used. In the case of the NCS data, the deviation was partly attributed to final-state effects; an estimate of those effects however could not yield any agreement with the predicted values. Thus, this large deviation between the calculated and measured effective temperatures in AC remains an open question.

VI. CONCLUSIONS

We have shown that the NRPS technique using 4.1-MeV bremsstrahlung can be used to measure the effective temperature of amorphous carbon by photoexciting the two nuclear levels at 3089 and 3684 keV in ^{13}C . The result is, however, strongly dependent on the radiative width of the nuclear levels and a high accuracy in the level width is required to achieve good accuracy in T_s . The measured value is close to those measured using the NCS method. It is not clear however, why the effective temperatures obtained by the present and the NCS methods yield much higher values than those calculated using the VDOS. Thus, the deviation

between the measured and predicted values of T_s in graphite and amorphous carbon is not understood.

Finally, the same method may be used to measure the effective temperatures of highly oriented pyrolytic graphite (HOPG) in directions parallel and normal to the graphite planes. Such a measurement requires longer running times because of the need to use a natural sample of HOPG which contains only 1.11% ^{13}C .

ACKNOWLEDGMENTS

This research was supported by the German-Israeli Foundation for Scientific Research and Development (GIF) and by the Deutsche Forschungsgemeinschaft (DFG). Thanks are due to E. Wagner, W. Namyslak, H. Hollick, and their staff (IfS, Stuttgart) for their invaluable assistance during the course of this work.

-
- ¹R. Moreh, W. C. Sellyey, and R. Vodhanel, *Phys. Lett.* **92B**, 286 (1980).
- ²R. Moreh, W. C. Sellyey, D. C. Sutton, and H. Zabel, *Phys. Rev. B* **35**, 821 (1987).
- ³F. Ajzenberg-Selove, *Nucl. Phys. A* **506**, 1 (1990).
- ⁴R. Moreh, O. Beck, I. Bauske, W. Geiger, R. D. Heil, U. Kneissl, J. Margraf, H. Maser, and H. H. Pitz, *Phys. Rev. C* **48**, 2625 (1993).
- ⁵H. Rauh and N. Watanabe, *Phys. Lett.* **100A**, 244 (1984).
- ⁶M. P. Paoli and R. S. Holt, *J. Phys. C* **21**, 3633 (1988).
- ⁷J. M. Mayers, T. M. Burke, and R. J. Newport, *J. Phys. Condens. Matter* **6**, 641 (1994).
- ⁸O. Shahal and R. Moreh, *Phys. Rev. Lett.* **40**, 1714 (1978).
- ⁹R. Moreh and O. Shahal, *Surf. Sci.* **177**, L963 (1986).
- ¹⁰R. Moreh, O. Shahal, and V. Volterra, *Nucl. Phys. A* **262**, 221 (1976).
- ¹¹R. Moreh, S. Melloul, and H. Zabel, *Phys. Rev. B* **37**, 10 754 (1993).
- ¹²F. R. Metzger, *Prog. Nucl. Phys.* **7**, 53 (1959).
- ¹³T. Chapuran, R. Vodhanel, and M. K. Brussel, *Phys. Rev. B* **22**, 1420 (1980).
- ¹⁴W. E. Lamb, *Phys. Rev.* **55**, 190 (1939).
- ¹⁵W. A. Kamitakahara, *J. Phys. Chem. Solids* **57**, 671 (1996).
- ¹⁶R. Moreh, D. Levant, E. Kunoff, *Phys. Rev.* **45**, 742 (1992).
- ¹⁷G. E. Ewing and G. C. Pimentel, *J. Chem. Phys.* **35**, 925 (1961).
- ¹⁸J. C. Burford and G. M. Graham, *Can. J. Phys.* **47**, 23 (1969).
- ¹⁹U. Kneissl, H. H. Pitz, and A. Zilges, *Prog. Part. Nucl. Phys.* **37**, 349 (1996).
- ²⁰J. A. Young and J. U. Koppel, *J. Chem. Phys.* **42**, 357 (1965).
- ²¹R. M. Nicklow, N. Wakabayashi, and H. G. Smith, *Phys. Rev. B* **5**, 4951 (1972).
- ²²R. Al-Jishi and G. Dresselhaus, *Phys. Rev. B* **26**, 4515 (1982).
- ²³N. Pietralla, I. Bauske, O. Beck, P. von Brentano, W. Geiger, R.-D. Herzberg, U. Kneissl, J. Margraf, H. Maser, H. H. Pitz, and A. Zilges, *Phys. Rev. C* **51**, 1021 (1995).